On the Induction Period of Drop Breakup behind Shock Wave

V. M. Boiko[1, a)], A. V. Minakov[2, b)], S. V. Poplavski[1, c)], and A. A. Shebeleva[2]

[1] *Khristianovich Institute of Theoretical and Applied Mechanics SB RAS, Institutskaya str., 4/1, Novosibirsk, 630090, Russia*
[2] *Siberian Federal University, 660041, Krasnoyarsk, Russia*

[a)]Corresponding author: bvm@itam.nsc.rus
[b)] tov-andrey@yandex.ru
[c)]poplav@itam.nsc.ru

Abstract. The work is devoted to the experimental and numerical study of the dynamics and destruction of water droplets in the air flow behind incident shock wave in the Weber number range We = 150-2350. The structure of the flow near and in the wake of the drop is studied, the streamline features are established that determine the type of evolution of the drop form characteristic of these breakup modes and the erosion character. Comparison of the results of numerical simulation with experiments on the morphology of the drop was performed, as well as on dynamics, deformation, and the induction delay of breakup. Good agreement between calculations and experiments on the main characteristics of the process is shown.

INTRODUCTION

Aerodynamic dispersion of liquids is used in various technologies, where high demands are placed on the productivity of nozzles and the dispersed composition of sprays, and in particular, dispersion of liquids is a critical process in power engineering, aircraft and rocket engine construction. The most important task for engineering practice is to determine the necessary conditions for obtaining a spray with specified particle sizes. The laws of acceleration, deformation and destruction of liquid droplets under the action of aerodynamic forces have been studied for more than 100 years, and this subject remains relevant up to now. The results of numerous experimental studies of the aerodynamic droplets breakingup are quite fully reflected in a number of overviews (see, for example, [1-4]), where characteristic modes of crushing are described, indicating the ranges of their existence. As the main criteria of fragmentation the Weber numbers $\mathrm{We} = \theta U^2 d / o$ and Ohnesorge $\mathrm{Oh} = \mu_l / (\theta_l o d)^{0.5}$ were used. They reflect the

relationship between the aerodynamic force and, respectively, the surface tension force and the viscous friction force (ρ and U are the gas density and velocity, d is the droplet diameter, σ, ρ_l, μ_l are the surface tension, density and viscosity of the liquid).

A large number of different classifications of droplet crushing regimes are known. According to the most cited one [1], six main modes are distinguished: the vibrational, the bag, the bag and stamen, the breakdown of the surface layer, the rupture of the crests of the waves, the catastrophic crushing. Other crushing modes are known, for example, multimode breakup regimes [4], bag-plume and plume-shear modes [5]. In the classification proposed by Gelfand et al. [3, 6] in 1981, there are only three main modes of fragmentation: I mode includes modes of vibration, bag, bag and stamen, chaotic crushing (10 <We <40); II mode - destruction with erosion of the surface layer of the liquid (40 <We <10^3); III regime - explosive decay of droplets (10^3<We<10^5).

Theofanous et al. in [7] proposed to simplify the classification by isolating only two modes of fragmentation according to the physical mechanism of the instability of the interface between the liquid and gas phases: RTR (Rayleigh-Taylor piercing) 10 <We <100 and SIE (shear-induced entrainment) at We>100. RTR includes the bag-type crushing, the bag and stamen type, multimode crushing, chaotic crushing, etc., which are explained by the Rayleigh-Taylor instability. The SIE mode involves the disruption of the surface layer of liquid with subsequent stripping (sheet stripping, sheet-thinning) and the spraying of liquid stripped from the crests during the development of the Kelvin-Helmholtz instability in shear flows.

An analysis of the various studies shows that there are considerable discrepancies in the choice of the main crushing mode and in the estimation of the critical values of We_{kr}. Reason is in complexity of the experimental study, when, due to the transient nature of the gas-drops interaction, it is difficult to determine the shape of the droplets, their velocity, to establish the moments of the onset of fracture and complete crushing with an acceptable accuracy. It is noted [3-8, 11] that up to the present time there are many incomplete experimental data in the literature, an inaccurate description of the details of the phenomenon, a large scatter and unjustified arbitrariness in specifying the criteria for the destruction of We_{kr} are observed. Therefore, the problem of further accumulation and analysis of the experimental material on droplets breakup in high-speed flows remains urgent.

Another actual problem is the construction of a physical model of dispersion of liquids by aerodynamic forces. The problem is extremely complicated, since it requires simultaneous solution of problems on external and internal flows under non-trivial boundary conditions. It should be noted that since the year 2000 there has been an increased interest in the problem of numerical modeling of the disintegration of liquid films and jets, as well as the secondary crushing of droplets.

The only universal tool for calculating the primary sputtering of liquid jets is direct numerical simulation (DNS) with full resolution of the interphase boundary. This method can only be used for a very few tasks because of the huge computational costs. A computational method based on a combination of the VOF method for resolving interphase boundaries, LES models for describing turbulent flows and the technology of adapted movable grids to the boundary can be considered as a real alternative to previous approach. This technique allows us to correctly describe the behavior of the moving boundary and the main turbulent scales that participate in the atomization of the liquid, and are less demanding on computational resources. However, the described computational approaches require further development and testing for application in applied problems.

Thus, the development of an effective and reliable numerical methodology for describing the dispersion of liquids in high-gradient flows is a very urgent objective. The most effective testing of numerical technology is modeling in the calculation of the conditions realized in shock wave experiments and comparing the results with the maximum number of parameters. These can be integral quantitative parameters, such as the dynamics of acceleration and deformation of a drop [9,10], the period of induction of destruction [11]. This may include structural features that indicate the flow patterns of the droplet, the type of instability of its surface, and the deformation scenario, the physical mechanism of destruction, and the nature of the liquid erosion [11].

In this paper, we present the results of an experimental and computational study of deformation processes and aerodynamic crushing of drops of low-viscosity (Newtonian) liquids in shock waves (SH) in order to determine the type and characteristic induction time of droplet destruction in the little-studied range of Weber numbers We = 100 ÷ 2500, and also for comparison of calculations with experimental data.

EXPERIMENT

The experiments were performed in a shock tube UT-4M (ITAM SB RAS) in the range of the SW Mach numbers Ms = 1.1-1.6. The main characteristics of the installation: high-pressure chamber (HPC, length -1 m, internal section d = mm); accelerating section of the low pressure channel (LPC, length - 3 m, round section 64 mm); working section (length - 1.4 m, section square 52x52 mm^2); measuring section (length - 0.3 m, cross section - 52×52 mm^2), equipped with quartz windows 20×200 mm for shadow visualization and a drop entry device in free fall. HPC and LPC are separated by a high-speed electro-pneumatic valve to start the installation on a signal from the synchronization system. A single drop of water d = 2-3 mm crossed the laser synchronization beam on the way to the channel axis and triggered

the shock tube. The duration of the quasi-stationary flow behind the shock wave front is 500-700 microseconds [9, 10].

The dynamics of the interaction between droplets and hydrocarbons was recorded by the method of multi-frame shadow photography. The exposure time (≤ 50 ns), the interval between frames ($\Delta t = 30 \pm 0.1$ μs) and the number of frames (up to 20) were set by a laser stroboscope, and the spatial separation of the frames was performed by a waiting photoregistrator with a rotating mirror [8]. The received photographs (24x18 mm) were digitized, but not the whole frame. Just the most informative part of the frames was digitized in order to obtain a high resolution (Fig. 1). The gas parameters behind shock front were determined as a function of the Mach number of the shock wave $Ms = Vs / c$ in

the theory of shock waves, where *Vs* - is the front velocity, *c* - is the sound velocity ahead of the front [8-11]. The velocity of the SW front was measured in two ways: by moving the shock wave front on two adjacent frames of shadow images (frames 1 and 2 in Fig. 1, a and Fig. 1, b) from the time of the known base (270 mm) travel between two pressure sensors. Relative error of measurement of speed ~ 1%.

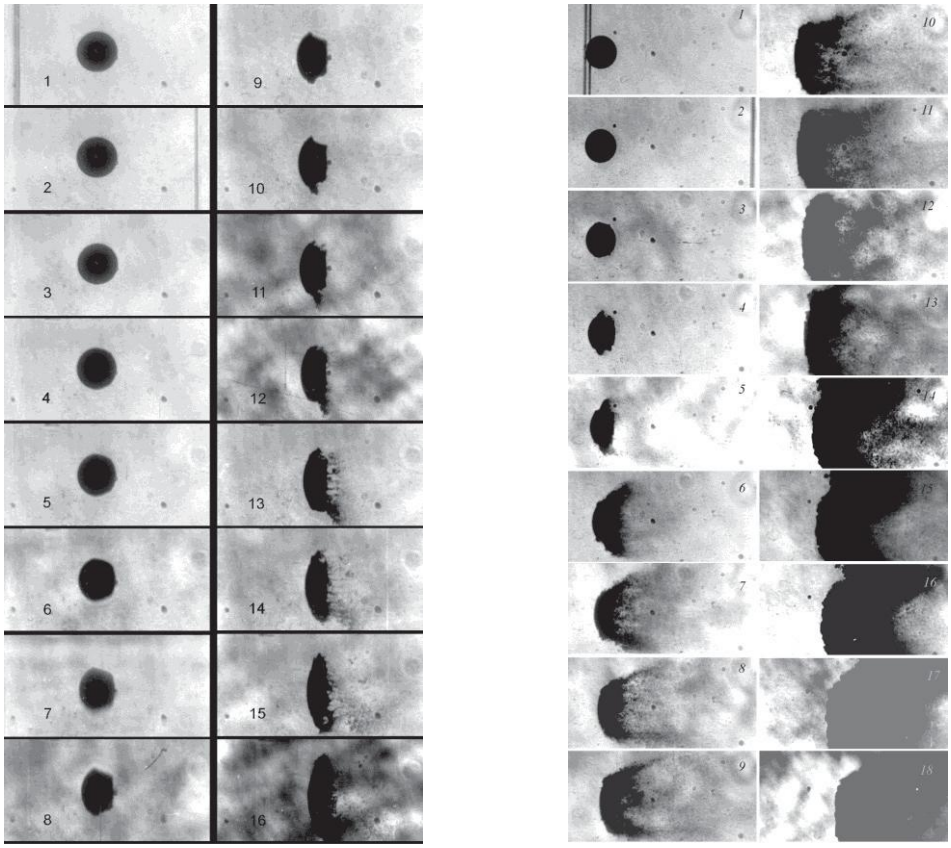

(a) (b)

FIGURE 1. Deformation and destruction of a drop of water in the flow behind the shock wave;
Water: $\rho_l = 10^3$ kg / m^3, o = $73 \cdot 10^{-3}$ N/m, $\mu_l = 10^{-3}$ N*s/m; air: $\rho_0 = 1.2$ kg/m^3.
(a) u = 82 m/s, d = 2.7 mm, We = 400; (b) u = 174 m/s, d = 2.9 mm, We = 2310, Δt = 30 μs,.

Figure 1 shows two characteristic series of frames, each of them is obtained in one experiment and illustrates the dynamics of acceleration, deformation and fragmentation of a drop in the air flow behind the shock wave. Fig. 1, a corresponds to the beginning, and Fig. 1, b - the end of the investigated range of Weber numbers. The nature and beginning of the destruction were determined visually. On the morphology of the windward surface with its smooth streamlined shape with a growing radius of curvature, the type of fracture of the drop at We = 400 (Fig. 1, a) corresponds to the classical breakdown of the surface liquid stratum, described in [4, 7, 11, 12]. There are all the signs of the liquid film separation from the droplet equator (frames 10-12); the film is destroyed on the strands, elongated along the gas flow (frames 13,14), and the crushing them latter into micro droplets (frames 14-15).

The beginning of destruction is the time when the crushing products appear in the wake of the drop (Fig. 1, a frame 11). The induction time for the destruction of t_{in} was determined by the time from the intersection by the front of the SW of the windward boundary of the drop (frame 1) to the appearance of crushing products (frame 11). The absolute accuracy of this data is limited to a half-interval between neighboring frames and is ≈ 15 μs.

As for the droplet destruction at We> 2000 (Fig. 2, b), the morphology of the windward surface becomes more complicated. Before the beginning of the destruction (frame 4), its shape is near to spherical and relatively smooth. Subsequently, the central part of the droplet nucleus flattens out, and characteristic waves appear on the periphery, which are associated with the development of the Kelvin-Helmholtz instability. In this mode, two mechanisms of

liquid erosion are observed simultaneously: crushing starts from the “sheet stripping” mechanism (frame 4), then the mechanism of “wave crests striping” from the windward surface of the drop is activated (frames 6,7).

The data on the times of induction of water droplet fracture are obtained in the Weber range We = 150 ÷ 2350, and it is established that in the whole investigated range the beginning of the droplet destruction is determined by one mechanism "sheet stripping". The measured delays t_{in}, depending on the flow velocity, are shown in Fig. 2, a. The data are presented in logarithmic coordinates and approximated with high accuracy by a straight line, the slope of which determines the exponent of the time dependence of the beginning of the droplet destruction on the flow velocity $t_{in} = 1{,}1 \bullet 10^4 U^{-1{,}33}$.

Figure 2, b shows the same data in the form of the dependence of the dimensionless induction time of the destruction t_{in}/t_0 on the Weber number, where $t_0 = (d_0/U)(\rho_l/\rho)^{0.5}$. Approximation in logarithmic coordinates determines the character of the dependence in the form $t_{in}/t_0 = 1{,}03\mathrm{We}^{-1/6}$.

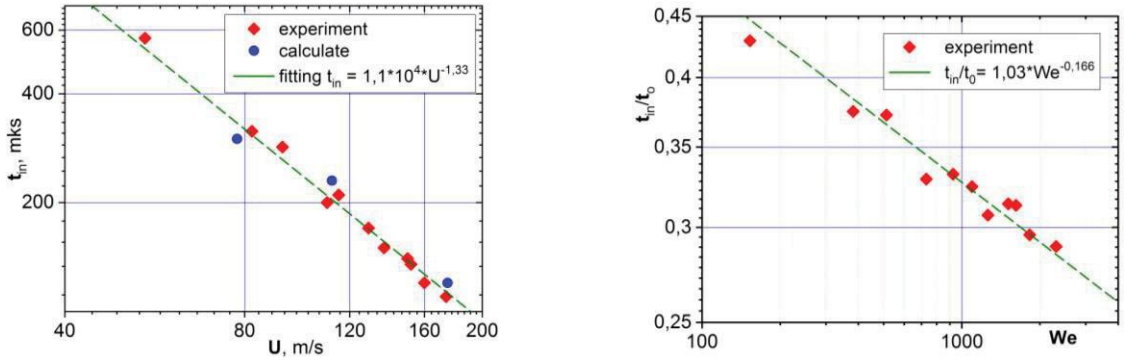

FIGURE 2. The induction time of water drop destruction depending on the flow velocity behind the shock front $t_{in}(U)$ (a) and on the Weber number t_{in}/t_0(We) (b)

For comparison, Fig. 3 also gives data from [3] on the induction time t_{in}/t_0 for Newtonian liquids in the range We = 10-140. There is a sharp change in the fracture mechanism at We ~ 150.

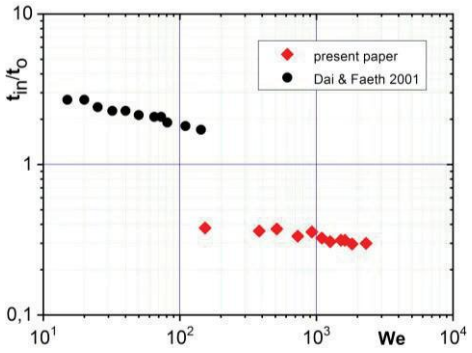

FIGURE 3. The dimensionless time of induction of the destruction of a drop of water as a function of Weber's number We

NUMERICAL ALGORITHM

The mathematical model of the secondary fracture of droplets is based on the VOF method [4].The idea of the method is that a fluid and a gas are regarded as a single two-component medium; the spatial distribution of phases within the calculation domain is determined by the special marker function. Since the free surface moves along with the liquid, the free boundary movement in the space is tracked by solving the transfer equation of liquid phase volume fraction in the cell. The CSF algorithm [5] was used to model the surface tension within the VOF method, the LES model [6] was used to model turbulence. The main features of numerical studies are described in [7-8].

The modeling of the destruction of water droplet in the flow behind the shock wave was carried out using the VOF method described above for different Weber numbers 220≤We≤2200 .The parallelepiped with dimensions 30×30×50 mm was the calculation area. The inlet condition with a fixed value of the velocity, determined from the value of the Weber number, was set on one of the parallelepiped faces. The outlet conditions were specified on the other faces of the calculation area. A spherical drop of water with the diameter d ~ 2-3 mm was placed at a distance of 5 mm from the entrance to the calculated region at the initial time. The shock wave passed and created an air flow, that acted on the droplet. A Cartesian uniform grid was used for the calculation. The detailing of that grid was 6.5 million nodes. However, methodological calculations have shown that such grid is not sufficient to resolve the interphase boundary of formed small droplets. Therefore, gradient adaptation of the computational grid technique was applied. In the calculation process, the grid automatically thickens in the region of large gradients. The gradient of the volume fraction of liquid in the cell was chosen as the control parameter. Cells in the region of high gradients are four times smaller than in the original grid. The total number of computed nodes in the calculation process was close to 15 million nodes in the optimized grid. The use of such a detailed mesh allowed to resolve the secondary droplets up to 20 μm in size.

The dynamics of the process that occurs when a shock wave interacts with a drop of water d = 2.75 mm is shown in Fig. 4.The gas flow velocity is 77.7 m / s, this corresponds to the Weber number We = 400, with the Mach number of the shock wave Ms = 1.14 and the Mach number of the stream M = 0.22. The interval between frames is 30 μs. The shock wave moves from left to right, deforming the drop.

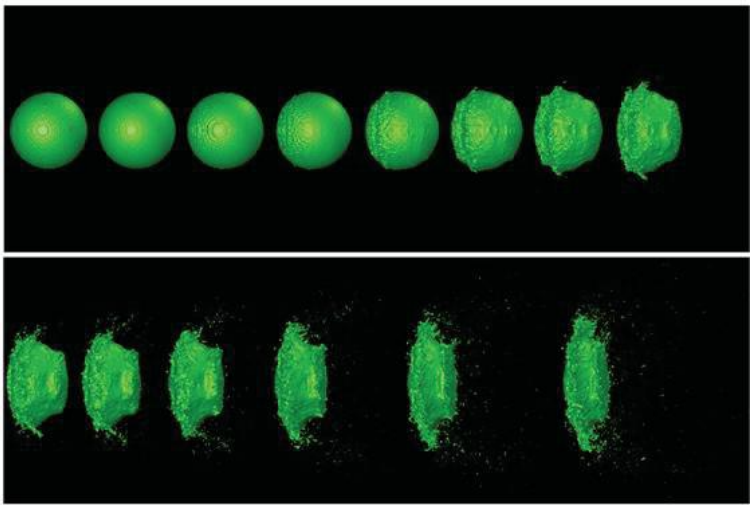

FIGURE 4. Dynamics of water droplet destruction when interacting with a shock wave for Weber number We = 400.

A comparison of the calculation with the experimental data (Fig.1, a) is shown in Fig. 5. As can be seen, the simulation results and experimental pictures coincide qualitatively in the shape of the interphase boundary and in dynamics at the similar time moments. That means that the computational algorithm has a good resolving power. The appearance of a film downstream is the first sign of the beginning of the destruction of a droplet. Based on the results of numerical simulation, it was established that the induction time for destruction was equal to 300 μs, which corresponds to the experimental data (Fig. 2, and calculate).

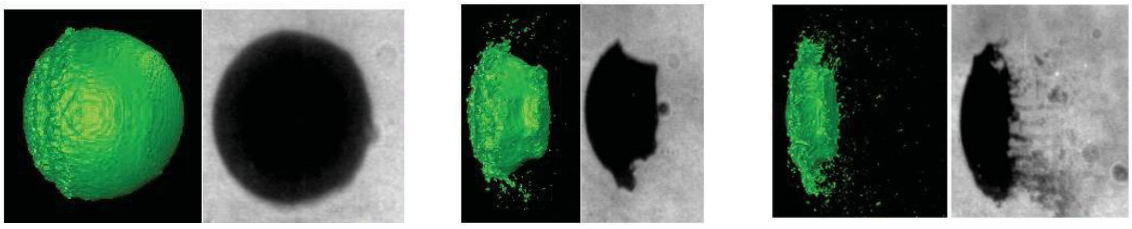

(a) (b) (c)

FIGURE 5. Comparison of the morphology of the drop in the experiment and calculations at the characteristic moments of residence in the flow behind the shock wave for Weber number We = 400: (a) t = 120 μs; (b) t = 270 μs, (c) t = 390 μs

SUMMARY

In the shock-wave experiment the “sheet stripping” type of water drops breakup in the Weber number range We = 150 ÷ 2500 was studied in detail by the method of shadow high-speed filming. The morphology of deformation and fragmentation of a drop is investigated. For the first time in this range, data were obtained on the time of onset of droplet destruction. The dependence of the induction time of fracture on the flow velocity behind shock wave frunt is revealed. It is established that the dimensionless induction time is inversely proportional to the Weber number to a power of 1/6.

A numerical simulation of the decay of individual water droplets in the flow behind the shock wave is carried out. The structure of the flow near and in the wake of the drop is studied; the flow patterns that determine the type of evolution of the shape characteristic of these modes and the character of the liquid erosion are established.

Comparison of the results of numerical simulation with experiments on the morphology of the drop, the dynamics of its acceleration, deformation, and the time delay of the liquid erosion are compared. The good agreement between calculations and experiments on the main characteristics of the process is shown.

ACKNOWLEDGMENTS

The work was carried out within the framework of the basic state task (project № 0323-2018-0010) and was funded by RFBR according to the research project № 18-38-00565.

REFERENCES

1. M. Pilch and C. A. Erdman, Int J Multiphase Flow **13(6)**, 741–757(1987).
2. G. M. Faeth, L. P. Hsiang and P. K. Wu, Int J Multiphase Flow **21**, 99–127 (1995)
3. B. E. Gelfand, Prog Energy Combust Sci. **22**, 201–265 (1996).
4. D. R. Guildenbecher, C. Lopez-Rivera and P. E. Sojka, Exp Fluids **46**, 371–402(2009)
5. Z. Dai, and G.M. Faeth, Int J Multiphas Flow **27**, 217-236 (2001)
6. A. A. Borisov, B. E. Gelfand, M. S. Natanzon, O. M. Kossov, J Engineering Phys and Thermophys **40**, 64-70 (1981)
7. T. G. Theofanous, V. V. Mitkin, C. L. Ng, C. H. Chang, X. Deng and S. Sushchikh, Phys. Fluids **24**, 022104 (2012)
8. V. M. Boiko, A. N. Papyrin, and S. V. Poplavskii, J. Appl. Mech. Tech. Phys. **28(2),** 263-269 (1987)
9. V. M. Boiko and S. V. Poplavski, Fluid Dynamics **42(3),** 433-441(2007)
10. V. M. Boiko and S. V. Poplavski. Combustion, Explosion, and Shock Waves **45(2),** 198–204 (2009)
11. V. M. Boiko and S. V. Poplavski, Combustion, Explosion, and Shock Waves **48(4),** 440–445 (2012)
12. A. A. Ranger and J. A. Nicholls, AIAA J. **7**, 285-290 (1969)
13. C. W. Hirt and B. D. Nichols, J. Comput. Phys. **39**, 201–226 (1981)
14. J. U. Brackbill, D. B. Kothe, and C. A. Zemach, J. Comput. Phys. **100**, 335– 54 (1992)
15. J. Smagorinsky, Month. Wea. Rev. **91,** 99–164 (1963)
16. A. A. Gavrilov, A. V. Minakov, A. A. Dekterev, and V. Y. Rudyak , J. of Appl. and Industrial Mathem.. 559-568. (2011)
17. A. V. Minakov, V. Y. Rudyak, A. A. Gavrilov, and A. A. Dekterev, Thermophys. Aeromech. **19**, 385–395 (2012)